



ELSEVIER

Physica A 213 (1995) 41–49

**PHYSICA A**

## Large scale simulations of the two-dimensional Cahn–Hilliard model

Raúl Toral<sup>a,1</sup>, Amitabha Chakrabarti<sup>b</sup>, James D. Gunton<sup>c</sup>

<sup>a</sup> *Departament de Física, Universitat de les Illes Balears, 07071 Palma de Mallorca, Spain*

<sup>b</sup> *Department of Physics, Kansas State University, Manhattan, KS 66506, USA*

<sup>c</sup> *Department of Physics, Lehigh University, Bethlehem, PA 18015, USA*

---

### Abstract

We review some recent numerical studies of the Cahn–Hilliard model in two dimensions, for phase separation with different values of the minority area fraction  $\phi$ . We find that dynamical scaling is satisfied at sufficiently late times for the pair correlation function, the structure factor and the droplet distribution function. We study how the shape of these scaling functions change with the area fractions and compare these results with available theoretical predictions. The time dependence of the characteristic length is consistent with an asymptotic growth law exponent  $1/3$  for all area fractions.

---

The process of phase separation that many mixtures, such as binary alloys, undergo, when quenched from a high-temperature, homogeneous state to a point below the coexistence curve, has been the subject of many experimental, theoretical and numerical studies [1]. The subsequent evolution is greatly determined by the location of the quench inside the phase diagram. In the classical picture, the so-called spinodal line divides the phase diagram according to the kind of instability that might govern the dynamical process. For small volume fraction,  $\phi$ , of the minority component, when the system is quenched between the spinodal and the coexistence lines, the system is unstable against localized, strong amplitude concentration fluctuations. In this situation, nuclei of the minority phase are formed. These nuclei evolve with time in such a way that they would dissolve if their typical linear size is less than a certain critical length, and grow otherwise. In the spinodal decomposition region the system is unstable against long wave-length, small amplitude concentration fluctuations, which generate a deeply

---

<sup>1</sup> Author to whom all correspondence should be sent. E-mail= raul@hp1.uib.es, tel: +34-71-173235, fax: +34-71-173426.

interconnected pattern that coarsens with time. Although this simple picture is of general validity, one can not sharply separate the two regions below the coexistence curve, and the spinodal line merely serves as an indication to which process dominates [2,3].

While a complete understanding of this phase separation process, especially for the late-time behavior, is still lacking, numerical simulations have had a long tradition in studying this problem and have served as a useful guide to theoretical developments. In the Cahn–Hilliard model [4], the basic ingredient is a conserved concentration field  $\psi(\mathbf{r}, t)$  representing the difference in concentration of the two components of the mixture. The time evolution of this field is given by the following equation:

$$\frac{\partial \psi(\mathbf{r}, t)}{\partial t} = \frac{1}{2} \nabla^2 [-\psi + \psi^3 - \nabla^2 \psi] \quad (1)$$

This complicated partial differential equation has so far defied analytical solutions valid for arbitrary time  $t$ . It seems, at this point, that the only way to extract reliable information concerning the late time behavior is by numerical studies. In this paper we review some of our work [5,6] on numerical studies of the Cahn–Hilliard equation in two dimensions. An extensive three-dimensional study including quenches for several values of the volume fraction is still lacking. One has to realize that the numerical integration of the Cahn–Hilliard equation is very demanding in computer resources, even for two-dimensional systems, because the system has to evolve long enough time in order to reach the scaling regime and, as time increases, finite size effects become important if the system size is not large enough. The numerical studies proceed by discretising space by using a regular lattice of  $N = L^2$  points and mesh size  $\delta x$ . We have chosen a mesh size  $\delta x = 1.0$  for the Laplacian discretization on a square lattice of sizes varying between  $N = 540^2$  for area fraction  $\phi = 0.05$  and  $256^2$  for  $\phi = 0.21$ . With this choice for  $\delta x$  we have found that droplets are circular in shape, whereas larger choices for  $\delta x$  produce anisotropic growth of droplets that reflect the underlying symmetry of the square lattice used in the numerical discretization.

In Fig. 1 we show two typical configurations for two different values of the area fraction  $\phi$ . For  $\phi = 0.50$ , Fig. 1a, the initial field configuration was chosen to be random and uniformly distributed in the interval  $[-1, 1]$ . Note the presence of the deeply interconnected pattern characteristic of spinodal decomposition. For the smaller area fraction,  $\phi = 0.21$ , Fig. 1b, one introduces strong concentration fluctuations by considering that the initial field is Gaussian distributed around the mean value  $\psi_0 = 1 - 2\phi$  and a variance of magnitude 5. Note that the irregular droplets evolve towards circular shapes at the late stages. Similar circular droplets are seen for  $\phi = 0.05$ .

The structure formation in the system during the phase separation process is analyzed in terms of the normalized time-dependent structure factor  $s(\mathbf{k}, t)$ :

$$s(\mathbf{k}, t) \equiv \frac{S(\mathbf{k}, t)}{\langle \psi^2(t) \rangle - \langle \psi \rangle^2} = \frac{\langle \frac{1}{N} |\sum_{\mathbf{r}} e^{-i\mathbf{k}\cdot\mathbf{r}} [\psi(\mathbf{r}, t) - \langle \psi \rangle]|^2 \rangle}{\langle \psi^2(t) \rangle - \langle \psi \rangle^2} \quad (2)$$

We also compute the pair-correlation correlation function,  $g(\mathbf{r}, t)$  defined as the Fourier transform of  $s(\mathbf{k}, t)$ . The above normalization procedure allows us to make a more

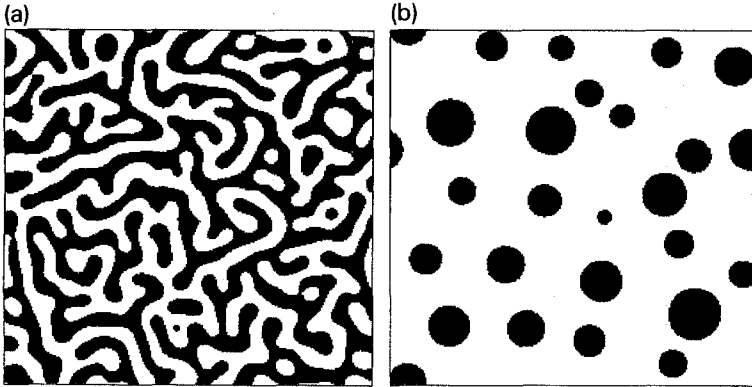


Fig. 1. (a) Typical configuration from the numerical solution of the two-dimensional Cahn–Hilliard equation for area fraction  $\phi = 0.50$ . Black (white) regions denote a positive (negative) value for the field  $\psi(r, t)$ . (b) typical configuration for  $\phi = 0.21$ .

reasonable comparison of the shape of the scaling functions for different area fractions, since the magnitude is normalized even though  $\langle \psi \rangle$  is different for different area fractions.

As a measure of the domain size, we have used the location of the first zero of the correlation function. This is denoted by  $R_g(t)$ . In experimental studies for which the structure function is more directly accessible one uses instead the inverse of the location of its maximum,  $k_m$ . However, the lattice discretization used in the numerical studies makes it difficult to determine  $k_m$  precisely, and  $R_g(t)$  can be determined much more accurately. Since at late stages clusters are circular in shape, the average radius of gyration also provides a reliable measure of the characteristic domain size.

An important development in the last several years [1,7,8] is the understanding that the late stages of the phase separation process in various binary mixtures is characterized by one dominant length scale,  $R(t)$ , proportional to the average size of the domains. One of the few exact results in this field, the classical result of Lifshitz and Slyozov [9], applicable when the volume fraction of one of the components of the mixture is vanishingly small, predicts that the average domain size (as given by the mean value of the minority phase droplet radius) behaves as  $R(t) \sim t^{1/3}$ . This asymptotic  $t^{1/3}$  growth-law has been extended for larger values of the concentration [10]. Due to the existence of only one length scale, the late stage evolution of the system can be described in terms of scaling with  $R(t)$ . Scaling implies that the circularly averaged pair correlation function and structure function depend on time through  $R(t)$  only. Namely:

$$g(r, t) = \mathcal{G}(r/R(t)), \quad s(k, t) = R(t)^d \cdot \mathcal{F}(kR(t)) \quad (3)$$

where  $\mathcal{G}(\rho)$  and  $\mathcal{F}(x)$  are time-independent scaling functions. In order to establish the universality classes of this scaling description, it is important to determine whether and how the growth law and the scaling functions change as one varies the area fraction.

In Fig. 2 we show the scaling functions for three values of the area fraction. It is

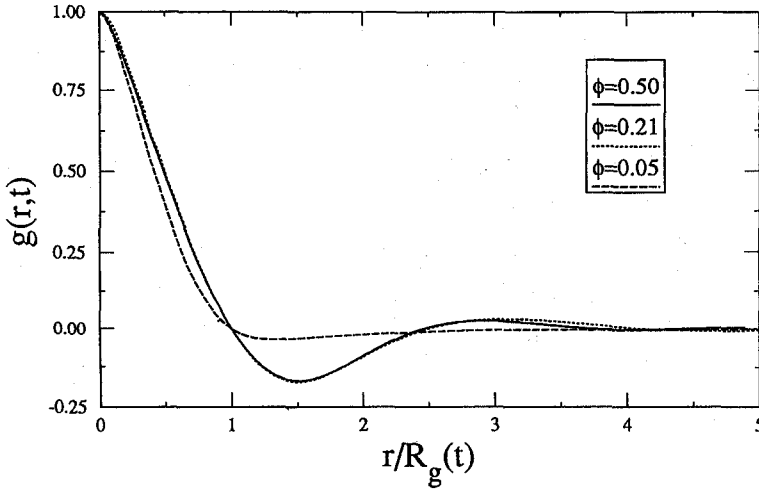


Fig. 2. Plot of the normalized pair-correlation function  $g(r, t)$  vs  $r/R_g(t)$  for three different values of the area fraction  $\phi = 0.50, 0.21, 0.05$ , to check the scaling ansatz in Eq. (3). The result for  $\phi = 0.50$  is taken from Ref. [23]. From this figure it is clear that the scaling function varies little between  $\phi = 0.50$  and  $\phi = 0.21$  whereas it changes significantly for  $\phi = 0.05$ .

interesting to note that, despite the big change in morphology (see Fig. 1), for  $\phi = 0.5$  and  $\phi = 0.21$ , there is little change in the scaling functions, whereas the corresponding scaling function for  $\phi = 0.05$  is clearly different from the others. The scaling function has also to be proven to be unaltered if one considers a concentration dependent diffusion coefficient [11]. The interesting feature of the scaling function for  $\phi = 0.05$  is that the oscillations seen in the scaling function for larger volume fractions are almost absent here and the magnitude of the pair correlation function is very small for  $r > R_g$ . This suggests that the spatial correlations among the droplets are much weaker in this case, in agreement by theoretical predictions of Mazenko [12], although we note that Mazenko's results have only been worked out explicitly for three-dimensional systems.

In Fig. 3 we plot the scaling functions for the unnormalized structure factors  $S(k, t)$ . We observe that there is a strong dependence of the scaling function on the area fraction. For instance, the maximum of the structure factor decreases with the area fraction. These features are in good qualitative agreement with a recent theory by Tokuyama, Enomoto and Kawasaki [13] although a complete quantitative comparison with theory is very difficult since the theory breaks down for area fractions larger than  $\phi = 0.10$ .

A detailed quantitative comparison can be made to the semiempirical model of Fratzl and Lebowitz [14]. In this model, the scaling functions are constructed in two stages: (1) the pair correlation scaling function is, in principle, modeled by the oscillatory decreasing function  $e^{-\lambda r} \sin(r\delta)/(r\delta)$  where  $\lambda$  is a constant proportional to the amount of the total interface present per unit area and  $\delta$  is another constant related to the typical domain size. (2) In order to incorporate the fact that, under very general circumstances, the structure function should behave as  $k^4$  for small values of  $k$ , the second stage consists of multiplying the Fourier transform of the above expression by the function

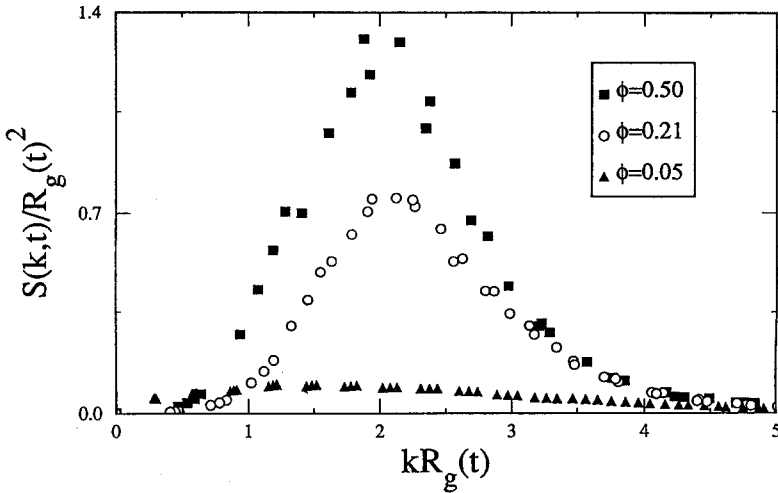


Fig. 3. Comparison of the scaling function obtained from the *unnormalized* structure factor  $S(k, t)$  with  $R_g(t)$  as the scaling length for various values of the area fraction.

$a_2 x^4 / (x^4 + c_2)$ ,  $a_2$  and  $c_2$  being two constants. The final expression for the scaling function  $\mathcal{F}(x)$  is then (in 2 dimensions):

$$\mathcal{F}(x) = \frac{a_2 x^4}{x^4 + c_2} \left( (3 + y^2) [y + (3 + y^2)^{1/2}] \right)^{-1/2} \quad (4)$$

where  $y = (x^2 - 1) / b_2 - 1 + d_2$  and  $d_2$  and  $b_2$  are constants depending on  $\lambda$  and  $\delta$ .

There are, in principle, four parameters in the above theory. Two of them can be eliminated by requiring that the scaling function  $\mathcal{F}(x)$  attains a maximum of value unity at  $x = 1$ . That allows to eliminate two parameters, say  $a_2$  and  $c_2$  in terms of the other two. When comparing with simulation data, this rescaling procedure is also necessary in order to eliminate possible dependence of the scaling function on the particular scaling length chosen. We are, then, left with two parameters,  $b_2$  and  $d_2$  to fit the data. This two-parameter fit, however, is not free of problems because, as mentioned before, it is difficult to accurately determine the maximum of the numerically determined scaling function  $\mathcal{F}(x)$ . Once this axes-rescaling has been performed, a least squares fitting of expression (4) to the simulation data yields the following values for the parameters:  $b_2 = 0.391$ ,  $d_2 = 0.644$  for  $\phi = 0.50$ ;  $b_2 = 0.383$ ,  $d_2 = 0.932$  for  $\phi = 0.21$  and  $b_2 = 2.196$ ,  $d_2 = 0.528$  for  $\phi = 0.05$  (in this latter case of  $\phi = 0.05$  only values satisfying  $x \geq 1$  have been included in the fit). Following Fratzl and Lebowitz, and considering that the value for  $d_2$  is not very critical for the fit, we can also fix the value of  $d_2$  to be a constant ( $d_2 = 0.6$ ) independent of the area fraction, and consider  $b_2$  to be the only adjustable parameter. A least squares fit in this case yields  $b_2 = 0.387$ ,  $0.371$ ,  $2.377$  for  $\phi = 0.50$ ,  $0.21$ ,  $0.05$ , respectively. These values again confirm that the variation between the scaling functions for  $\phi = 0.50$  and  $\phi = 0.21$  is very small. Fig. 4 compares the scaling function  $\mathcal{F}(x)$  with the theoretical prediction

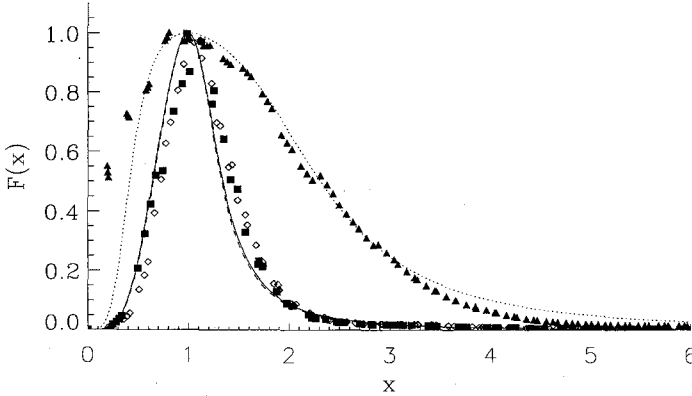


Fig. 4. Comparison of the scaling function for the structure factor with the semi-empirical model calculation of Fratzl and Lebowitz [14]. Same symbols than in Fig. 3. Here we take the constant value  $d_2 = 0.6$ . The parameter  $b_2$  is changed as follows:  $b_2 = 0.387$  (solid line),  $0.371$  (dashed line),  $2.377$  (dotted line). See the text for an explanation of these parameters.

for the latter values of the parameters mentioned above. The general agreement is rather good except, perhaps, for intermediate values of the scaling variables where the theoretical prediction is systematically larger than the simulation data and, in the case of  $\phi = 0.05$  also for small values of the scaling variable  $x$ .

One can define the function  $f_R(R, t)$  as the probability distribution function of droplet radius  $R$  at time  $t$ . If  $R(t)$  is some given measure of the relevant system length (for instance, the mean droplet radius), the corresponding probability density function for the variable  $x_0 = R/R(t)$  is  $f_{x_0}(x_0, t) = R(t)f_R(R, t)$ . The dynamical scaling hypothesis affirms that this function is independent of time, for late enough times, i.e.:  $f_{x_0}(x_0, t) = f_{x_0}(x_0)$ . We have checked that scaling is reasonably satisfied at late times ( $t > 4000$ ) both for area fractions  $\phi = 0.21$  and  $\phi = 0.05$ . The dynamical scaling for the cluster distribution function is obtained in the classical theory of Lifshitz and Slyozov, valid in the limit of vanishingly small volume fraction for three-dimensional systems. This theory neglects the spatial interaction between droplets. Many attempts have been made to systematically include the correlation among droplets in some approximate way in the theoretical calculations both for two and three-dimensional systems. The main features of these extensions is that the  $t^{1/3}$  growth-law is unaltered but the shape of the droplet distribution function varies depending on the assumptions made. We now briefly review some of the main theoretical results.

Rogers and Desai [15] carry out a simple extension of Lifshitz-Slyozov theory in two dimensions. However, in two dimensions, there seems to be no consistent steady-state result in the limit of  $\phi \rightarrow 0$ . In the non-steady-state calculation for  $\phi \rightarrow 0$ , Rogers and Desai found an explicit scaling form for the droplet distribution function which we will loosely call the "Lifshitz-Slyozov (LS)" scaling function in two dimensions. The theory of Ardell [16] includes the effect of diffusive correlations among nearest-neighbor clusters by introducing an ad hoc cutoff limit in the diffusion geometry. In

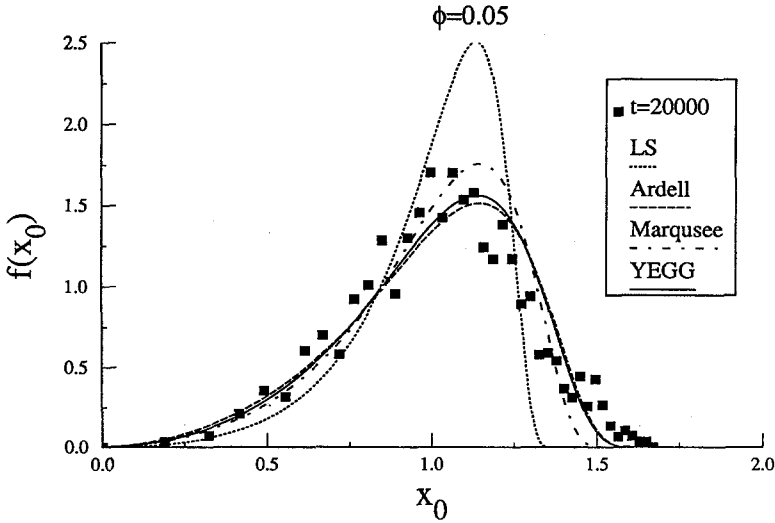


Fig. 5. Simulation data for droplet distribution function at the latest time ( $t = 20000$ ) for  $\phi = 0.21$  compared with various theories.

the limit of  $\phi \rightarrow 0$ , one also recovers the LS scaling form. For finite area fraction, the scaling function needs to be evaluated numerically. In Marqusee's theory [17], the surrounding droplets are considered as an "effective medium", the distribution function is derived in a self-consistent fashion and it needs to be evaluated numerically. Zheng and Gunton [18] have extended the previous theory by using a new expansion parameter (instead of  $\phi^{1/2}$  used by Marqusee). However, the range of validity of this theory is beyond the numerical simulations presented here since the authors expect that their scheme breaks down for  $\phi > 0.01$ . In the mean-field approach of Yao, Elder, Guo and Grant [19], many droplet correlation effects are approximated in the same manner as the Thomas-Fermi approach for a Coulombic system. The authors found that, in two dimensions, their theory breaks down for area fraction  $\phi > 0.085$  when the screening length is close to the average radius of droplets.

In Fig. 5 we compare the predictions of different theories with the numerical data for volume fraction  $\phi = 0.05$ . From this figure we find that the LS scaling function is sharper and much higher in the peak than the corresponding numerical data. These discrepancies are expected since, as mentioned earlier, the LS results are only valid in the limit of zero volume fraction. For  $\phi = 0.05$  we find that the data agrees reasonably well with the predictions of Yao et al and Ardell (actually the difference between these two theories is very small except near the peak). We note that there are small differences between the theoretical predictions and the numerical data both near the peak and the tail of the distribution. It seems that the location of the maximum is slightly different in the numerical distribution function. Since the uncertainties in the numerical results are larger near the tail of the distribution, it is difficult to judge whether the discrepancy near the tail is real or not. For area fraction  $\phi = 0.21$ , Marqusee's theoretical result

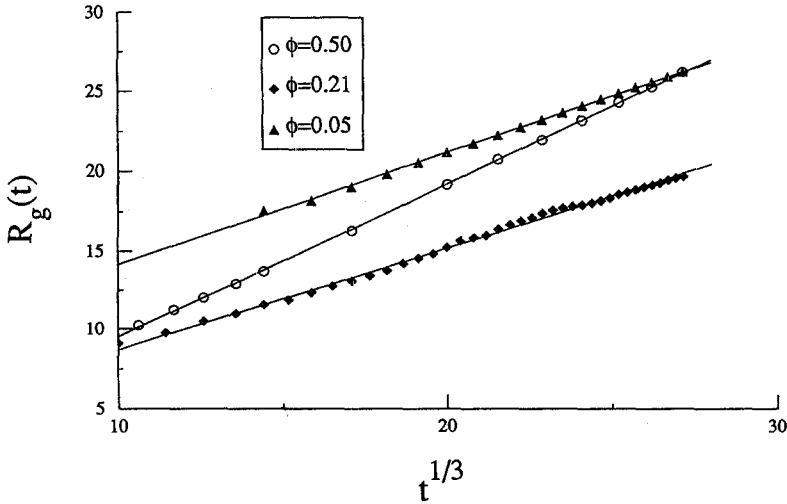


Fig. 6. The characteristic domain size  $R_g(t)$  is plotted against  $t^{1/3}$  for various area fractions  $\phi$ . The solid lines are best fit to the data. The result for  $\phi = 0.50$  is taken from Ref. [23]

comes close to the simulation results. However, there appears to be some systematic differences between the data and the theory. It seems, then, that a complete theoretical description of the late-stage growth process in two dimensions is still incomplete and we hope that our numerical work would direct attention to this direction.

We now turn our attention to the growth-law governing the characteristic domain size. The classical Lifshitz-Slyozov theory, based on a mechanism of evolution governed by bulk diffusion across the interfaces, predicts that the average droplet size behaves as  $t^{1/3}$ . This theory has been qualitatively extended by Huse [10] to the case of equal volume fraction of the two phases. On the other hand, the extensions to the Lifshitz-Slyozov theory mentioned before predict that the growth-law exponent remains unaltered. For critical quenches, it has been well established in the literature both by analytical calculations [20] and by large-scale computer simulations [21–23] that the asymptotic growth law exponent is  $1/3$ . In Fig. 6 we find that the data for  $R_g(t)$  can be fitted by a straight line against  $t^{1/3}$  for three different area fractions, thus confirming that the asymptotic growth law exponent is  $1/3$ . We can conclude that the growth exponent remains the same when the area fraction changes from a small value to the critical concentration.

We acknowledge financial support from the Dirección General de Investigación Científica y Técnica, contract number PB 92-0046 (Spain). This work was partially supported by NSF grant No. DMR-9100245 and a grant of computer time at the Pittsburgh Supercomputing Center. Acknowledgment is also made to the Donors of the Petroleum Research Fund, administered by the American Chemical Society for partial support of this work. We thank Drs. E. Gawlinski, Hong Guo, J. Viñals and Qiang Zheng for providing us with their numerical results.



**References**

- [1] J.D. Gunton, M. San Miguel and P.S. Sahni, in: *Phase Transitions and Critical Phenomena*, Vol. 8, edited by C. Domb and J.L. Lebowitz (Academic, London, 1983).
- [2] K. Binder in *Materials Science and Technology*, Vol. 5 : *Phase Transformation in Materials*, ed. P. Haasen (VCH, Weinheim, Germany 1990), p. 405.
- [3] A. Chakrabarti, *Phys. Rev. B* 45 (1992) 9620.
- [4] J.W. Cahn and J.E. Hilliard, *J. Chem. Phys.* 28 (1958) 258.
- [5] R. Toral, A. Chakrabarti and J.D. Gunton, *Phys. Rev. B* 39 (1989) 901; *Phys. Rev. A* 45 (1992) R2147.
- [6] A. Chakrabarti, R. Toral and J.D. Gunton, *Phys. Rev. A* 44 (1991) 12133; *Phys. Rev. E* 47 (1993) 3025.
- [7] K. Binder and D. Stauffer, *Phys. Rev. Lett.* 33 (1974) 1006.
- [8] J.L. Lebowitz, J. Marro and M.H. Kalos, *Act. Metall.* 30 (1982) 290, and references therein.
- [9] I.M. Lifshitz and V.V. Slyozov, *J. Phys. Chem. Solids* 19 (1961) 35.
- [10] D.A. Huse, *Phys. Rev. B* 34 (1986) 7845.
- [11] A.M. Lacasta, J.M. Sancho, A. Hernández-Machado and R. Toral, *Phys. Rev. B* 45 (1992) 5276; *Phys. Rev. B* 48 (1993) 6854.
- [12] G.F. Mazenko, *Phys. Rev. Lett.* 63 (1989) 1605; *Phys. Rev. B* 43 (1991) 5747.
- [13] M. Tokuyama, Y. Enomoto and K. Kawasaki, *Physica A* 143 (1987) 183.
- [14] P. Fratzl and J.L. Lebowitz, *Acta Metall.* 37 (1989) 3245; P. Fratzl, *J. Appl. Cryst.* 24 (1991) 593.
- [15] T.M. Rogers and R.C. Desai, *Phys. Rev. B* 39 (1989) 11956.
- [16] A.J. Ardell, *Phys. Rev. B* 41 (1990) 2554; *Acta Metall.* 20 (1972) 61.
- [17] J.A. Marqusee, *J. Chem. Phys.* 81 (1984) 976.
- [18] Q. Zheng and J.D. Gunton, *Phys. Rev. A* 39 (1989) 4848.
- [19] J.H. Yao, K.R. Elder, H. Guo and M. Grant, *Phys. Rev. B* 45 (1992) 8173 and McGill University Preprint.
- [20] A.J. Bray, *Phys. Rev. Lett.* 62 (1989) 2841.
- [21] R. Toral, A. Chakrabarti and J.D. Gunton, *Phys. Rev. Lett.* 60 (1988) 2311; A. Chakrabarti, R. Toral and J.D. Gunton, *Phys. Rev. B* 39 (1989) 4386.
- [22] T.M. Rogers, K.R. Elder and R.C. Desai, *Phys. Rev. B* 37 (1988) 9638.
- [23] E.T. Gawlinski, J. Viñals and J.D. Gunton, *Phys. Rev. B* 39 (1989) 7266.